PROCEEDINGS OF SCIENCE

# Scattering Observables from Few-Body Densities and Application in Light Nuclei

**Alexander Long*** **and Harald W. Grießhammer**

*Institute for Nuclear Studies, Department of Physics,*
*George Washington University, Washington DC 20052, USA*

*E-mail:* alexlong@gwu.edu, hgrie@gwu.edu

The dynamics of scattering on light nuclei is numerically expensive using standard methods. Fortunately, using recent developments, the relevant quantities can be factored into a product of the $n$-body transition density amplitude (TDA) and the interaction kernel of a chosen probe. These TDAs depend only on the target, and not the probe; they are calculated once and stored. The kernels depend on only the probe and not the target; they can be reused for different targets. The calculation of transition densities becomes numerically difficult for $n \geq 4$, but we discuss a solution through use of a similarity renormalization group transformation, and back transformation. This technique allows for extending the TDA method to $^6$Li. We present preliminary results for Compton scattering on $^6$Li and compare with available data, anticipating an upcoming thorough studi [18]. We also discuss ongoing extensions to pion-photoproduction and other reactions on $A \leq 6$ nuclei.

*The 11th International Workshop on Chiral Dynamics (CD2024)*
*26-30 August 2024*
*Ruhr University Bochum, Germany*

*Speaker

 ISSN 1824-8039 . Published by SISSA Medialab.

## 1. Introduction

Effective Field Theories (EFTs) in nuclear physics make precise predictions by employing only those degrees of freedom that are most pertinent to the physical system under consideration, rather than relying on the complete set of intrinsic degrees of freedom present in the underlying theory (typically quarks and gluons in nuclear and particle physics). In this work, we utilize Chiral Effective Field Theory ( $\chi$EFT ) which adopts nucleons and pions as its fundamental degrees of freedom. The present study is concerned with scattering probes off light nuclei. To this end, the Transition Density Amplitude (TDA) method was developed by Grießhammer *et al.* and de Vries *et al.* [1, 17]. The TDA formalism describes the interaction of a probe with an $A$-body target. The process is factored into the interaction with $n$ nucleons which are therefore called *active* and the background $A-n$ nucleons which do not directly interact with the probe which are called *spectators*. The former enters in description of the kernel (along with the probe description) whereas the latter constitutes the TDA. Figure 1 provides an illustrative example for the case $A = 3$. The mathematical treatment of these two components is entirely distinct therefore if one has access to $a$ distinct kernels (e.g. Compton pion and scattering) and $b$ distinct TDAs (e.g. $^3$He, $^4$He, $^6$Li), then a total of $ab$ different outcomes may be generated (provided they are in the same kinematics). The $n$-body kernel characterizes the interaction in the reduced case where interacts exclusively with the $n$-body system. For example, the one-body kernel in Compton scattering encompasses the same contributions as those arising in Compton scattering off a single nucleon. The total scattering amplitude off an $A$-body nucleus is given by

$$A_M^{M'}(\vec{k},\vec{q}) = \left\langle M' \left| \binom{A}{1}\hat{O}_1(\vec{k},\vec{q}) + \binom{A}{2}\hat{O}_2(\vec{k},\vec{q}) + ... + \binom{A}{A}\hat{O}_A(\vec{k},\vec{q}) \right| M \right\rangle \tag{1}$$

where $\hat{O}_i$ is the $i$-body kernel, $M, M'$ is the spin projection of the target nucleus, and there are $\binom{A}{i}$ ways for a probe to interact with $i$ nucleons. Fortunately, $\chi$EFT provides small dimensionless expansion parameter $\delta \approx 0.4$ [3] which predicts a hierarchy of scales for probe energies greater than $\gtrsim$ 40MeV [20–22]. Therefore, the 3-body contribution and higher are negligible at this order, and we simply use

$$A_M^{M'}(\vec{k},\vec{q}) = \binom{A}{1}\langle M'|\,\hat{O}_3(\vec{k},\vec{q})\,|M\rangle + \binom{A}{2}\langle M'|\,\hat{O}_2(\vec{k},\vec{q})\,|M\rangle$$

In practice, this is enough for accuracy on roughly the 5% level [1].

## 2. Kernels and Densities

The one-body and two-body kernel must be considered separately. Their form is different, and they require a one- and two-body density respectively. Symbolically, the matrix element $\hat{O}_1$ is rather involved and can be found in Griesshammer *et al.* [1, 3]. The central result is that up to boost corrections it can be written as:

$$\left\langle M' \left| \hat{O}_1(\vec{k},\vec{q}) \right| M \right\rangle = \sum_{\substack{m_3^{s\prime} m_3^s \\ m_3^t}} \hat{O}_1\left(m_3^{s\prime} m_3^s, m_3^t; \vec{k},\vec{q}\right) \rho^{m_3^t M_T, M'M}_{m_3^{s\prime} m_3^s}(\vec{k},\vec{q})\ . \tag{2}$$

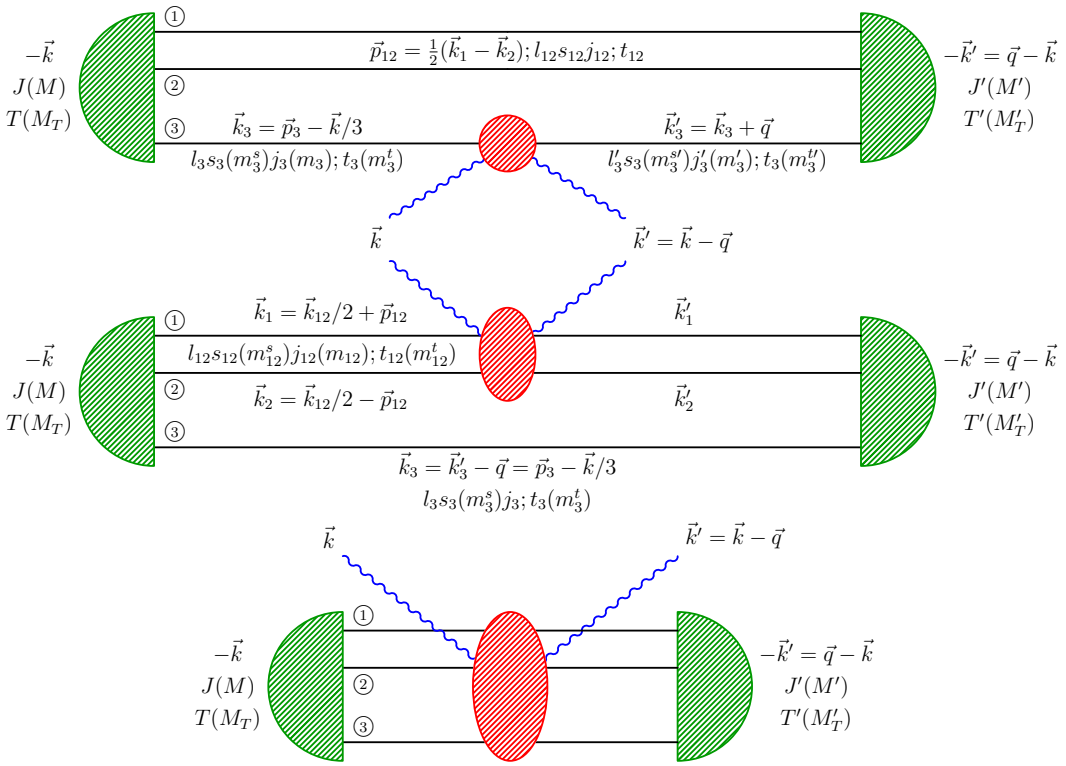


**Figure 1:** Kinematics in the center of mass frame and quantum numbers for an $A = 3$ system in the case of Compton scattering. Generalization to other reactions only changes the ingoing/outgoing probe. Generalization to $A > 3$ would result in more internal lines representing the nucleons. Top: one-body processes $\hat{O}_1$ (one active nucleon, two spectators), center: two-body processes $\hat{O}_2$ (two active nucleons, one spectator), bottom: three-body processes $\hat{O}_3$ (all nucleons active, no spectators). Red represents the kernels; everything else is represented by the densities. Green represents the wavefunction of the nucleons. $J(M)$ is the spin (projection) and $T(M_T)$ is the isospin (projection) of the nucleus. $l_i, s_i(m_i^s), j_i(m_i), t_i(m_i^t)$ refer to the angular momentum, spin angular momentum, total angular momentum, isospin (and their projections where appropriate) of the specific subsystem in the kernel being considered. From Grießhammer *et al.* [1]. *This is getting kind of wordy...*

Here $\rho$, is the *one-body transition density amplitude* (TDA) for the nucleus and can be interpreted as the probability amplitude that nucleon with isospin projection $m_3^t$ absorbs momentum $\vec{q}$, changes its spin projection from $m_s^3$ to $m_s^{3'}$ and changes the spin-projection of the nucleus from $M$ to $M'$, hence the name "Transition Density Amplitude". Additionally, $M_T$ is the isospin projection of the entire nucleus and $\vec{k}$ is the momentum of the incoming probe. The two-body case works similarly, and results in

$$\left\langle M' \left| \hat{O}_2 \right| M \right\rangle = \sum_{\alpha_{11}', \alpha_{12}} \int \mathrm{d}p_{12}\, p_{12}^2\, \mathrm{d}p_{12}'\, p_{12}'^2\, \hat{O}_2^{\alpha_{12}'\alpha_{12}}\left(p_{12}', p_{12}\right) \rho_{\alpha_{12}'\alpha_{12}}^{M_T, M'M}\left(p_{12}', p_{12}; \vec{q}\right) \tag{3}$$

Where

$$|\alpha\rangle = |\,[(l_{12}s_{12})j_{12}(l_3 s_3)j_3]\,JM,\ (t_{12}t_3)TM_T\rangle \tag{4}$$

This is the two-body equivalent to (2). The two-body density $\rho^{M_T,M'M}_{\alpha'_{12}\alpha_{12}}$ is of course distinct from the one-body density. Moreover, just like the one-body case, it can be interpreted as a transition probability density amplitude. It depends on the incoming and outgoing quantum numbers $\alpha_{12}$ and $\alpha'_{12}$ of the system of the two active nucleons, and also on their initial and final relative momenta $p_{12}$ and $p'_{12}$ (also of the two nucleons) which are integrated over. As a result, the file size for the two nucleon TDAs is approximately 20 MB per energy and angle, whereas those of the one nucleon TDAs are on the order of a few KB. Importantly, the densities $\rho$ can for a given momentum transfer $\vec{q}$ be computed directly from a nuclear potential, such as the chiral Semilocal Momentum-Space ($\chi$SMS) potential [2] without reference to the kernel $\hat{O}_1$ or $\hat{O}_2$.

## 3. SRG Transformation

Previous work using the TDA formalism has analyzed $^3$He and $^4$He [1, 3], but to extend this to $^6$Li involves more interactions and as a result the calculation is more complicated and computationally expensive. To make the calculation of a TDA feasible for $A > 6$, a *Similarity Renormalization Group* (SRG) transformation is employed [4, 15]. This is of much experimental interest since $^6$Li is a stable solid at room temperature and is therefore relatively simple to conduct an experiment on. There has been some experiments on$^6$Li [10, 11], yet to date there is no theory prediction. We seek to fill in this gap. When using nuclear potentials, we approximate the nucleon-nucleon potential to be zero beyond a certain cutoff $\Lambda_{\mathrm{NN}}$, and consequently neglect contributions above this cutoff in our calculations. In general, a nuclear potential, such as the $\chi$SMS potential [2] does not fall off rapidly at high momenta. As a result we would have to extend the cutoff $\Lambda_{\mathrm{NN}}$ which in turn significantly increases the computational cost. The SRG transformation is a unitary transformation that shifts the relevant physics into the low-momentum region, thereby lowering minimum effective $\Lambda_{\mathrm{NN}}$ in the SRG evolved space. This, in turn, significantly improves the convergence rate of calculations for $A = 6$ making them actually possible. The SRG transformation can be thought of as a local averaging or smoothing of the potential, resulting in decreased "resolution" as the SRG is applied, however it does this without losing any of the underlying information or compromising the physics. In the under-evolved, high resolution panel, fig. 2a, the potential does not go to zero rapidly at large momenta, whereas it does once the transformation is applied in the right panel, fig. 2b. As a result, a cutoff can be made at $\Lambda_{\mathrm{NN}} = 2\mathrm{fm}^{-1}$ without losing much accuracy, whereas the under-evolved potential required at least $\Lambda_{\mathrm{NN}} = 5\mathrm{fm}^{-1}$. The time complexity is at a minimum proportional to the number of array elements present, therefore we gain at least a factor of $(5/2)^2 = 6.25$ in efficiency; in practice the gains are even higher because near-zero values of the potential at large momenta means sparser grids can be used there. The SRG transformation is essential, but it also creates a change in the physical meaning of the free variables. In fact, any unitary transformation ($U^\dagger U = \mathbb{1}$) also transforms the coordinates:

$$\langle p' | V | p \rangle = \langle p' | U^\dagger U V U^\dagger U | p \rangle = \langle p' | U^\dagger \left( U V U^\dagger \right) U | p \rangle = \langle \widetilde{p}\,' | V_{eff} | \widetilde{p} \rangle = V_{eff}(\widetilde{p}, \widetilde{p}\,') \quad (5)$$

So referring to the free variables in an SRG-transformed potential as "momenta" is, to some extent, incorrect. They do not represent physical states in the sense that they are not eigenstates to physical momenta. The Lagrangeans that generate the Feynman diagrams in the kernel, however, depend

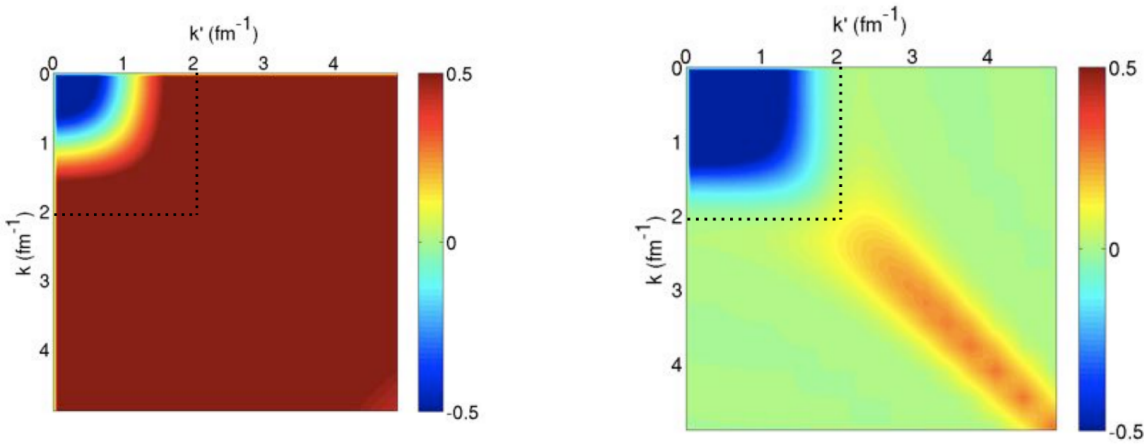


**(a)** High Resolution (before much SRG is applied)

**(b)** Low Resolution (evolved)

**Figure 2:** Nuclear potentials $V(k, k')$. Figures from Kai Hebeler: "Chiral Effective Field Theory and Nuclear Forces: overview and applications" presentation at TALENT school at MITP 2022, and modified with permission from Furnstahl *et al.* [15].

on physical momenta, and therefore we cannot directly use an SRG evolved potential in the non-SRG evolved kernel. To solve this, previous work with SRG transformations has transformed the Lagrangeans - and therefore the kernels - into the SRG evolved space as well. However, in the context of the density formalism this would mean adding SRG dependence into the kernel, thereby breaking kernel-density independence. This is undesirable since it means more work for the group developing the kernel; in particular it would mean one would have to transform the kernel with the SRG corresponding to the density every time a new SRG evolved density is applied. Additionally, the SRG transformation can take many different forms [4, 15]; we wish to allow for these developments without having to re-write the kernel code. Therefore, we developed a method whereby we first perform an SRG, then compute the densities via the SRG evolved potential, and then apply an inverse SRG transformation to the densities [16].

The process of completing the SRG evolution of the potential, solving for the wavefunction, and then applying the inverse transformation has parameters that must be fine-tuned, but this allows for uncertainty estimation. TDA calculations involving an SRG transform are done in the no-core shell model [26]. This involves the selection of a characteristic width $\omega_H$ and expansion in basis states. When expanded to infinite order, this basis forms a complete set, however, we truncate this expansion by only including excitations up to $N_{\text{tot}}$. Therefore, we can estimate the convergence of the expansion by comparing calculations for different values of $N_{\text{tot}}$ since at $N_{\text{tot}} = \infty$ the associated uncertainty goes to zero. The parameter $\Lambda_{\text{SRG}}$ represents the progression of the SRG evolution of the potential, as seen in figure 2 with $\Lambda_{\text{SRG}} = \infty$ corresponding to no evolution. As we will see all of these parameters effect the resulting cross-section.

Unfortunately the application of the SRG transformation is not strictly unitary, and therefore generates induced many-body forces. Our method neglects these forces, so it is essential to test their impact. We therefore utilize Compton scattering as a test-bed, and compare results using TDAs

calculated with and without the SRG transformation before moving to the more inovolved $^6$Li where we only have access to the SRG transformed TDAs. Fortunately figure 3 shows the uncertainty associated with these induced forces is small. During the TDA calculation, we obtain the binding energy of the simulated system, which we can use calibrate our parameters through comparison to the known experimental value. We determine an optimal $\omega_H$ that yields a good binding energy, while $N_{\text{tot}}$ is taken as large as feasible. With this benchmark established, we have extended our analysis to $^6$Li, for which only the SRG evolved form is accessible. Future investigations [18] will carefully assess the extent to which different $\Lambda_{\text{SRG}}$ values effect results.

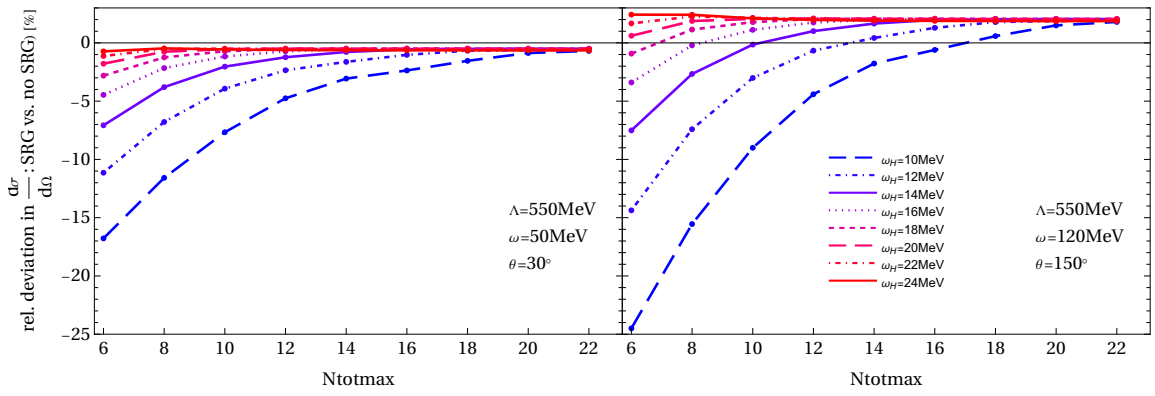


**Figure 3:** $^4$He Compton scattering SRG convergence, comparing the exact, vs SRG evolved approaches. Deviations are due to induced manybody forces. "Relative deviation, (Rel. deviation) of $A$ from $M$":= $\frac{A}{M} - 1$

In figure 3, we see the effectiveness of the results in the $^4$He case. We expect the deviation to decrease as $N$ increases, and importantly for our analysis, this shows what value of $N$ is required. The small error present at high $N_{\text{tot}}$ is present do to the induced many body forces.

### 3.1 Results for $^6$Li

The kernels used for $^6$Li Compton scattering are the same as Grießhammer *et al.* uses in $^3$He and $^4$He Compton scattering [1, 3]. Long *et al.* [18] will provide a full analysis of uncertainty. For this analysis an overall 10% uncertainty is assumed in agreement with Grießhammer *et al.* [1, 3] which accounts for the cutoff $\Lambda_{\text{NN}}$ and $\Lambda_{\text{SRG}}$ variation, along with $\omega_H$ selection. We include an additional, independent, contribution from $N_{\text{tot}}$ which is easy to calculate, but is negligible compared to other sources; the methodology behind this will be discussed in Long *et al.* [18].

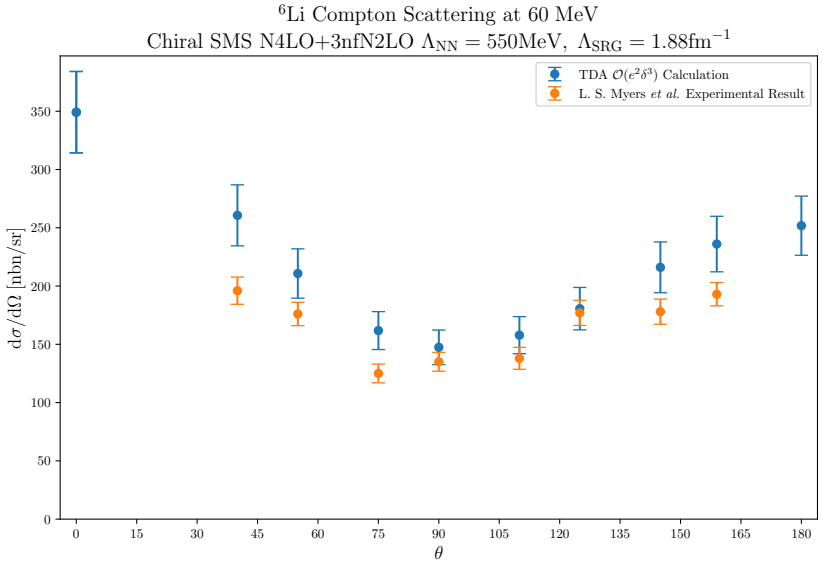


**Figure 4:** Compton scattering on $^6$Li as compared to Myers *et al.* [11].

The data presented here is promising but leaves room for improvement. The overall angle dependence of the TDA calculation is correct but the values appear to be off a constant offset. In Long *et al.* we will conduct a full uncertainty analysis, involving the $\Lambda_{NN}$ dependence, along with the order by order theory convergence and perhaps most importantly the convergence in the $\Lambda_{SRG}$ transform. Lastly we must note that experimental normalization issues cannot be ruled out.

## 4. Using TDAs in different processes

With the TDAs calculated for Compton scattering, we now wish to recycle them for new processes. In particular pion-photoproduction, and pion scattering are of interest. Fortunately their kernels share remarkable similarity since if one ignores the type of incoming/outgoing particle the processes are topologically identical.

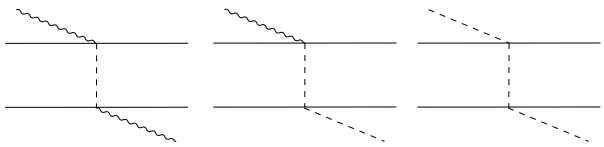

**Figure 5:** Topologically identical contributions to the twobody kernels of Compton scattering, pion-photoproduction, and pion scattering.

### 4.1 Pion-Photoproduction

For the pion-photoproduction one-body kernel, we use the results from single-nucleon scattering, $\gamma N \rightarrow \pi N$ which has been studied extensively both in $\chi$EFT and phenomenologically

[5, 7, 13, 14]. Its differential cross section can be decomposed into the electric and magnetic multipoles $E_{l\pm}, M_{l\pm}$ [5]. Over the years, many experiments have measured these multipoles to high order and with good precision [6]. The resulting scattering matrices $\mathcal{M}$ are exactly what enters as $\hat{O}_1$ in equation (2). This approach solves a significant problem since the calculation of the one-body pion-photoproduction kernel to high accuracy directly from Feynman diagrams requires including many terms in the chiral expansion due to the proximity of the $\Delta(1232)$ resonance at $\sim$ 200MeV. A theoretical prediction of these multipoles is given by Rijneeven et al [7], which we intend to compare to experimental data.

The two-body contributions do not easily decompose into multipoles, so we perform the calculation through expansions in the chiral Lagrangean via calculation of Feynman diagrams. To this end Beane *et al.* [23] provides the kernel for the reaction on the deuteron at threshold and since we only go up to the two-body kernel this is sufficient for our needs. Additionally this reaction kernel has been analyzed by Lenkewitz *et al.* [8, 9] whose result for $^3$He we now compare to. In particular, we consider the commonly referred to form factors $F_S^{S\pm V}, F_L^{S\pm V}, F_{T/L}^{(a)} - F_{T/L}^{(b)}$, a full description of these formfactors is present in Lenkewitz *et al.* [8]. Note that here we present only the central values, but upcoming work will provide a full analysis [19]. We use the $\chi$SMS potential, whereas Lenkewitz used the AV-18 potential, so it is expected our values will differ slightly.

| $^3$He Compton Scattering | Lenkewitz *et al.* AV-18 [8] | $\chi$SMS TDA calculation[19] |
|---|---|---|
| One-body | | |
| $F_T^{S+V}$ | 0.017(13)(3) | -0.017±uncertainty t.b.a |
| $F_T^{S-V}$ | 1.480(26)(3) | 1.48 ±uncertainty t.b.a |
| $F_L^{S+V}$ | -0.079(14)(8) | -0.005 ±uncertainty t.b.a |
| $F_L^{S-V}$ | 1.479(26)(8) | 1.48 ±uncertainty t.b.a |
| Two-body | | |
| $F_T^{(a)} - F_T^{(b)}$ | -29.3 fm$^{-1}$ | -29.4 fm$^{-1}$ ±uncertainty t.b.a |
| $F_L^{(a)} - F_L^{(b)}$ | -22.9 fm$^{-1}$ | -22.9 fm$^{-1}$ ±uncertainty t.b.a |

**Table 1:** $^3$He pion photoproduction form factor central values. Full analysis of uncertainty in Long *et al.* [19]

### 4.2 Pion scattering and other reactions

Beane *et al.* have developed the pion scattering kernel at threshold for both one-body and two-body interactions [12]. We anticipate extending this analysis to finite energy the targets $^3$H, $^3$He, $^4$He, $^6$Li. Once the pion-photoproduction and pion scattering kernels have successfully been developed, we will be able to calculate all of these reactions on previously analyzed targets in the density formalism since we already have produced most of the TDAs required. Our study will complement and expand on work by Braun *et al.* [24] by performing a thorough analysis of theory uncertainties for a range of chiral potentials as well as taking the first step to explore even heavier nuclei with pions.

## 5. Conclusion

We have described a comprehensive framework for computing scattering observables in light nuclei by factorizing the full amplitude into target-dependent few-body transition density amplitudes (TDAs) and probe-dependent interaction kernels. This work expands on work in refs, as well as work on few body targets [1, 3, 9]. This separation allows us to treat the nuclear structure and the reaction mechanism independently, thereby streamlining the calculation of observables. The central thrust of this work is the successful extension of the density formalism to heavier targets like $^6$Li by incorporating a similarity renormalization group (SRG) transformation. The SRG not only accelerates the convergence of our calculations by lowering the effective momentum cutoff, but—when combined with an appropriate inverse transformation of the densities—also preserves the kernel–density independence that is crucial for the versatility of our approach. We have presented preliminary results for Compton scattering on $^6$Li which disagrees slightly with data, showing the need for further analysis. We have outlined the ongoing efforts at extending the formalism to other reactions, such as pion-photoproduction and pion scattering on light nuclei [18, 25]. The ability to plug in different reaction kernels into the same TDA framework and vice versa not only enhances the predictive power of our approach but also paves the way for a unified treatment of various scattering processes in a wide range of few-body systems. Ultimately, this framework provides a promising route toward high-precision theoretical predictions, deepening our understanding of nuclear dynamics in light nuclei. *We wrote here "More in upcoming articles [18]....", what did we mean by this? To me this feels like a good place to end it.*

## 6. Acknowledgements

We thank Andreas Nogga and Xiang-Xiang Sun of FZ Jülich, whose work on producing the required TDAs we deeply appreciate. Our appreciation goes out to G. Feldman of the Myers *et al.* [10, 11] experimental collaboration for information about $^6$Li Compton experiments. We also thank organisers and participants Chiral Dynamics Bochum. This work was supported in part by the US Department of Energy under contract DE-SC0015393. Additional funds were provided by an Enhanced Student Travel Award of the Columbian College of Arts and Sciences of George Washington University. The computations of nuclear densities were performed by A. Nogga and X.-X. Sun on Jureca of the Jülich Supercomputing Centre (Jülich, Germany).

## References

[1] H. W. Grießhammer, J. A. McGovern, A. Nogga, and D. R. Phillips, "Scattering Observables from One- and Two-body Densities: Formalism and Application to $\gamma^3$ Scattering," *Few-Body Systems*, vol. 61, no. 4, Nov. 2020. DOI: 10.1007/s00601-020-01578-w.

[2] P. Reinert, H. Krebs, and E. Epelbaum, "Semilocal momentum-space regularized chiral two-nucleon potentials up to fifth order," *The European Physical Journal A*, vol. 54, no. 5, May 2018. DOI: 10.1140/epja/i2018-12516-4.

[3] Grießhammer, H.W., Liao, J., McGovern, J.A. et al. Compton scattering on with nuclear one- and two-body densities. Eur. Phys. J. A 60, 132 (2024). https://doi.org/10.1140/epja/s10050-024-01339-x arXiv:2401.16995.

[4] S. Szpigel and R. J. Perry, "The Similarity Renormalization Group,", Quantum Field Theory: A Twentieth Century Profile, Sep. 2000. https://doi.org/10.48550/arXiv.hep-ph/0009071

[5] R. L. Walker, "Phenomenological Analysis of Single-Pion Photoproduction," *Phys. Rev.*, vol. 182, no. 5, pp. 1729–1748, Jun. 1969. DOI: 10.1103/PhysRev.182.1729.

[6] R. L. Workman, M. W. Paris, W. J. Briscoe, and I. I. Strakovsky, "Unified Chew-Mandelstam SAID analysis of pion photoproduction data," *Phys. Rev. C*, vol. 86, no. 1, p. 015202, Jul. 2012. DOI: 10.1103/PhysRevC.86.015202.

[7] N. Rijneveen, A. M. Gasparyan, H. Krebs, and E. Epelbaum, "Pion photoproduction in chiral perturbation theory with explicit treatment of the $\Delta(1232)$ resonance," *Phys. Rev. C*, vol. 106, no. 2, p. 025202, Aug. 2022. DOI: 10.1103/PhysRevC.106.025202.

[8] M. Lenkewitz, E. Epelbaum, H.-W. Hammer, and U.-G. Meißner, "Neutral pion photoproduction off $^3$H and $^3$He in chiral perturbation theory," *Physics Letters B*, vol. 700, no. 5, pp. 365–368, Jun. 2011. DOI: 10.1016/j.physletb.2011.05.036.

[9] M. Lenkewitz, E. Epelbaum, H.-W. Hammer, and U.-G. Meissner, "Threshold neutral pion photoproduction off the tri-nucleon to $O(q^4)$," *The European Physical Journal A*, vol. 49, no. 2, Feb. 2013. DOI: 10.1140/epja/i2013-13020-1.

[10] L. S. Myers, M. W. Ahmed, G. Feldman, A. Kafkarkou, D. P. Kendellen, I. Mazumdar, J. M. Mueller, M. H. Sikora, H. R. Weller, and W. R. Zimmerman, "Compton scattering from $^6$Li at 86 MeV," *Phys. Rev. C*, vol. 90, no. 2, p. 027603, Aug. 2014. DOI: 10.1103/PhysRevC.90.027603.

[11] L. S. Myers, M. W. Ahmed, G. Feldman, S. S. Henshaw, M. A. Kovash, J. M. Mueller, and H. R. Weller, "Compton scattering from $^6$Li at 60 MeV," *Phys. Rev. C*, vol. 86, no. 4, p. 044614, Oct. 2012. DOI: 10.1103/PhysRevC.86.044614.

[12] S. R. Beane, V. Bernard, E. Epelbaum, U.-G. Meißner, and D. R. Phillips, "The S-wave pion–nucleon scattering lengths from pionic atoms using effective field theory," *Nuclear Physics A*, vol. 720, no. 3–4, pp. 399–415, Jun. 2003. DOI: 10.1016/S0375-9474(03)01008-X.

[13] R. L. Workman, M. W. Paris, W. J. Briscoe, and I. I. Strakovsky, "Unified Chew-Mandelstam SAID analysis of pion photoproduction data," *Phys. Rev. C*, vol. 86, no. 1, p. 015202, Jul. 2012. DOI: 10.1103/PhysRevC.86.015202.

[14] W. J. Briscoe, A. Schmidt, I. Strakovsky, R. L. Workman, and A. Švarc, "Extended SAID partial-wave analysis of pion photoproduction," *Phys. Rev. C*, vol. 108, no. 6, p. 065205, Dec. 2023. DOI: 10.1103/PhysRevC.108.065205.

[15] R. J. Furnstahl and K. Hebeler, "New applications of renormalization group methods in nuclear physics," *Reports on Progress in Physics*, vol. 76, no. 12, p. 126301, Nov. 2013. DOI: 10.1088/0034-4885/76/12/126301.

[16] X.-X. Sun, H. Le, A. Nogga, and U.-G. Meißner, in preparation (2025).

[17] J. de Vries, C. Körber, A. Nogga, et al., "Dark matter scattering off He in chiral effective field theory," *Eur. Phys. J. C*, vol. 84, p. 1138, 2024. DOI: 10.1140/epjc/s10052-024-13477-z.

[18] Alexander Long, Harald W. Grießhammer, X.-X. Sun, H. Le, A. Nogga, in preparation (2025). Transition density amplitude calculation of $^6$Li to $O(e^2\delta^3)$

[19] Alexander Long, Harald W. Grießhammer, X.-X. Sun, H. Le, A. Nogga, in preparation (2025). Transition density amplitude calculation of pion photoproduction on light nuceli.

[20] H. W. Grießhammer, J. A. McGovern, D. R. Phillips, and G. Feldman, "Using Effective Field Theory to analyse low-energy Compton scattering data from protons and light nuclei," *Progress in Particle and Nuclear Physics*, vol. 67, no. 4, pp. 841–897, Oct. 2012. DOI: 10.1016/j.ppnp.2012.04.

[21] R. P. Hildebrandt, "Elastic Compton Scattering from the Nucleon and Deuteron," 2005. Available: arXiv:nucl-th/0512064.

[22] R. P. Hildebrandt, H. W. Grießhammer, and T. R. Hemmert, "Nucleon polarizabilities from deuteron Compton scattering within a Green's function hybrid approach," *The European Physical Journal A*, vol. 46, no. 1, pp. 111–137, Sep. 2010. DOI: 10.1140/epja/i2010-11024-y.

[23] S. R. Beane, V. Bernard, T.-S. H. Lee, U.-G. Meißner, and U. van Kolck, "Neutral pion photoproduction on deuterium in baryon chiral perturbation theory to order $q^4$," *Nuclear Physics A*, vol. 618, no. 4, pp. 381–401, Jun. 1997. DOI: 10.1016/S0375-9474(97)00133-4.

[24] J. Braun, "Effective Field Theories and Electromagnetic Properties of Light Nuclei," Technische University Darmstadt (Germany), Fachbereich Physik, Apr. 24, 2019.

[25] Scattering Observables from Few-Body Densities and Application in Light Nuclei, PhD proposal, Geo Wash U, August 2022

[26] H. Zhan, A. Nogga, B. R. Barrett, J. P. Vary, and P. Navrátil, "Extrapolation method for the no-core shell model," *Physical Review C*, vol. 69, no. 3, Mar. 2004. DOI: 10.1103/PhysRevC.69.034302.